exists for Si ($\epsilon=12.0$). Kohn,[7] noting this discrepancy, corrected the effective-mass formalism for deep donor states. Formally, this was done by dividing the wave function into two parts, an outer region where the effective-mass formalism is still valid, and an inner region where, since the dielectric constant is no longer a good concept, a new wave function is required. Kohn, in addition, used the observed E_D rather than the calculated E_D in the effective-mass theory.

A recalculation of the g values with the corrected wave functions has not been carried out. However, the effect of the corrected wave functions on the g value can be considered qualitatively. Since the electrons of deep-donor impurities are less influenced by the lattice, a g value between that calculated from the uncorrected effective-mass theory [Eqs. (4) and (5)] and the 2.0023 expected for a tightly bound s-like state would be predicted. In the case of the donor resonances in GaP, the g values are indeed between these limits.

As a final note, a comment on the linewidth and shape will be made. The wave function of the donor electron will, even with a radius of 7 Å, overlap several neighboring Ga and P nuclei. Since all Ga and P isotopes have a nuclear moment, there is a resultant hyperfine interaction between the donor electron and every nucleus overlapped by the electron. If the individual lines resulting from these hyperfine interactions are not resolved, an inhomogeneously broadened line is obtained. The width of 45–60 G is not inconsistent with unresolved hyperfine interactions with several neighboring Ga and P nuclei. However, an inhomogeneously broadened line would be expected to have a Gaussian rather than the observed Lorentzian shape. The observed Lorentzian shape is probably due to motional effects caused by hopping of electrons between donor impurities. If one uses the criterion observed in Ge and Si, hopping begins to occur when the average separation between donors is about fourteen times the Bohr radius. With a Bohr radius of 7 Å, hopping would therefore occur when the total donor concentration N_D is the order of 10^{18} cm^{-3}. The net donor concentration in the samples used in the resonance experiments was of this order, and hopping would therefore be expected.

ACKNOWLEDGMENTS

I would like to thank L. M. Foster, J. E. Scardefield, and M. R. Lorenz, who provided the samples, W. Fitzpatrick for aid in the resonance experiments, and J. F. Woods for useful discussions.

PHYSICAL REVIEW VOLUME 154, NUMBER 3 15 FEBRUARY 1967

De Haas–Van Alphen Effect and Fermi Surface in Arsenic*

M. G. PRIESTLEY†
Institute for the Study of Metals and Department of Physics, University of Chicago, Chicago, Illinois

AND

L. R. WINDMILLER‡, J. B. KETTERSON, AND Y. ECKSTEIN
Argonne National Laboratory, Argonne, Illinois

(Received 15 July 1966)

A detailed and accurate study of the de Haas–van Alphen effect and Fermi surface of arsenic has been made by a vector-modulation technique. We find two sets of Fermi surfaces which together give the required volume compensation. The first set contains three closed, centrosymmetric pockets (β in our notation) which have a tilt angle (for the minimum area) of $86.4\pm0.1°$ from the trigonal axis. Their total volume is found to be $(2.12\pm0.01)\times10^{20}$ carriers/cm^3. The other set forms a single multiply connected surface of symmetry $\bar{3}m$ and consists of six α pockets (the Berlincourt carriers) which have a tilt angle of $37.25\pm0.1°$, and which are connected together by six long thin necks with a tilt of $-9.6\pm0.1°$. This is in excellent agreement with the recent pseudopotential calculation by Lin and Falicov if the β pockets are due to electrons at L and the multiply connected surface to holes around T. The multiplicities of the pockets are deduced from the experimental data and are supported by the consequent satisfactory agreement with the observed electronic specific heat.

I. INTRODUCTION

ARSENIC is a semimetal with the same $A7$ trigonal crystal structure as the other semimetals bismuth and antimony.[1] Recent theoretical work by Cohen, Falicov, and Golin[2] has shown that all their band structures are primarily a function of this crystal structure, and so these semimetals should have many

* Supported by the National Science Foundation, the Advanced Research Projects Agency, and the U. S. Atomic Energy Commission.

† This work was begun during the tenure of a National Science Foundation predoctoral fellowship in the Institute for the Study of Metals and the Department of Physics, University of Chicago, Chicago, Illinois.

‡ Present address: University of Bristol, Bristol, England.

[1] R. W. G. Wyckoff, *Crystal Structures* (Interscience Publishers, Inc., New York, 1960), Vol. 1.

[2] M. H. Cohen, L. M. Falicov, and S. Golin, IBM J. Res. Develop. 8, 215 (1964).

common features. Detailed experiments have been made for Sb[3–5] and these agree very well with the results of a pseudopotential band-structure calculation by Falicov and Lin.[6] For bismuth the experimental situation is at last fairly clear[7,8] but theoretical work has been hampered by the large spin-orbit coupling.

In the case of arsenic the published experiments give only a partial picture of the Fermi surface and its relation to the band structure. The first experiments were made by Berlincourt[9] who studied the de Haas–van Alphen (dHvA) effect. He found two sets of carriers, one with very long periods of the order of $10^{-5}G^{-1}$ (γ in our notation; see Sec. III) and the other with short periods of $\sim 5\times 10^{-7}G^{-1}$ (α in our notation). He fitted the short periods to a number of ellipsoidal pockets related by the crystal symmetry and tilted by $\sim 35°$ from z in the yz plane. The long periods were assigned to a small pocket directed along the trigonal axis. It was noted that the required carrier compensation could not be obtained from these two carriers alone. Later, ultrasonic-attenuation experiments by Ketterson and Eckstein[10] (geometric resonance and quantum oscillations) and experiments by Shapiro and Williamson[11] on the quantum oscillations in the ultrasonic attenuation and on the dHvA effect showed the presence of another set of carriers (β in our notation) which could be used to provide volume compensation. The volume of each β pocket was determined in these experiments as 5.9–6.5×10^{19} electron/cm^3 but neither the number of pockets nor carrier compensation could be established. Ketterson and Eckstein's data[10] on the very long period suggested that the γ pocket had a small tilt angle of the order of 5° from the trigonal axis.

Cyclotron resonance in As has been studied by Datars and Vanderkooy.[12] Their data for this and the dHvA effect[12] are quoted as being in agreement with the tilted ellipsoid model for the α carriers proposed by Berlincourt.[9]

A pseudopotential calculation of the band structure by Falicov and Golin[13] enabled some conclusions about the carriers to be made but further identification was hindered by the lack of experimental data. It was therefore of considerable interest to apply to arsenic the new experimental techniques developed for the study of the dHvA effect in antimony.[3,4] The difficult experimental problem of producing unstrained single-crystal samples had already been solved.[10]

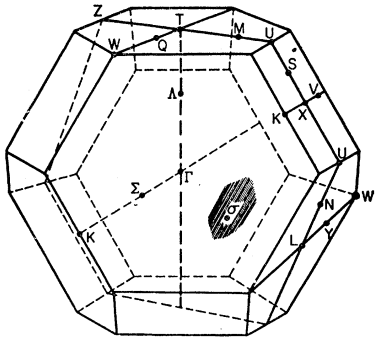

FIG. 1. The Brillouin zone for the $A7$ crystal structure. The standard notation (Ref. 2) for the symmetry points is used. With our sign convention for the angles in the yz plane (the same as Ref. 14), ΓT is at 0°, ΓX at $+59°17'$, ΓL at $-72°50'$ or equivalently $+107°10'$.

The wealth of new and accurate information obtained in the present experiment enables us to determine the number, arrangement, and volume of each of the pockets. This, in conjunction with the concurrent refinement of the pseudopotential band-structure calculation by Lin and Falicov,[14] fixes the location and sign of the carriers. It is shown below that nearly all details of the experiment and theory are in excellent agreement.

II. EXPERIMENTAL TECHNIQUES

The modulation technique and apparatus used are identical to those described in detail in Refs. 3 and 4. The sample is situated in a static magnetic field of up to 20 kG and a modulation field at a frequency of approximately 2 kc/sec is applied. The signal induced in a small pickup coil around the sample was filtered, amplified, and detected by a lock-in amplifier tuned to a harmonic of the modulation frequency. The resultant signal contains dHvA oscillations as a result of harmonic generation by the nonlinear susceptibility of the sample. The modulation field direction and pickup coil axis are not in general parallel to the steady field and the angles between them can be adjusted to take full advantage of the vector nature of each component of the oscillatory magnetization. All measurements were made at temperatures between 1.2 and 4.2°K.

The arsenic single crystals were prepared from the melt from Cominco 99.9999% stock by the techniques described in Ref. 10. The crystals were cut by a spark cutter into cylinders $\frac{1}{8}$-in. diam by $\frac{1}{4}$-in. long and were finally etched in hot aqueous KOH solution. Samples oriented to within 1° of the three principal axes were prepared and used in the experiment.

For accurate experiments on the semimetals it is essential that the orientation of the magnetic fields with respect to the crystal axes should be known to much better than 1°. This was achieved by using a specially designed back-diffraction x-ray camera accurate to 0.2°. Final trimming so that the field was rotated in the desired plane to $\pm 0.2°$ was accomplished by tilting the Dewar about either of two perpendicular horizontal

[3] L. R. Windmiller and M. G. Priestley, Solid State Commun. 3, 199 (1965).
[4] L. R. Windmiller, Phys. Rev. **149**, A472 (1966).
[5] W. R. Datars and J. Vanderkooy, IBM J. Res. Develop. **8**, 247 (1964).
[6] L. M. Falicov and P. J. Lin, Phys. Rev. **141**, 562 (1966).
[7] See J. B. Ketterson and Y. Eckstein, Phys. Rev. **137**, A1777 (1965), and references quoted therein.
[8] R. N. Bhargava, Bull. Am. Phys. Soc. **10**, 605 (1965).
[9] T. G. Berlincourt, Phys. Rev. **99**, 1716 (1955).
[10] J. B. Ketterson and Y. Eckstein, Phys. Rev. **140**, A1355 (1965).
[11] Y. Shapira and S. J. Williamson, Phys. Letters **14**, 73 (1965).
[12] W. R. Datars and J. Vanderkooy, Bull. Am. Phys. Soc. **10**, 110 (1965).
[13] L. M. Falicov and S. Golin, Phys. Rev. **137**, A871 (1965).
[14] P. J. Lin and L. M. Falicov, Phys. Rev. **142**, 441 (1966).

axes and utilizing the known symmetry of the oscillations.

Magnetic fields were measured directly by NMR to 1 part in 10^5, so dHvA periods could be measured to better than 0.1% except for the very long period, of order $10^{-5}G^{-1}$, where the small number of oscillations limited the accuracy to 0.2%. Periods were measured in this way at selected points and the remainder of the data was obtained from field-rotation measurements, with the modulation conditions adjusted so as to make the desired oscillatory component dominant.

III. RESULTS

The Brillouin zone for the arsenic structure is shown in Fig. 1. In presenting the results we follow the usual convention of labeling the mutually perpendicular binary (ΓK), bisectrix, and trigonal (ΓT) axes as the x, y, and z axes, respectively. The sign of angles measured from the trigonal axis in the yz plane is such that a positive rotation is from the direction ΓT towards that ΓX which lies in the first quadrant. It should be noted here that previous experiments have not determined the sign of the tilt angles in arsenic. The resolution of this ambiguity is discussed in Ref. 4.

A. The Long Periods

The data for the long periods in the yz plane are shown in Fig. 2. These oscillations are found down to approximately 600 G for the magnetic field **H** parallel to z. A series of careful determinations of the period for **H** along z, using direct NMR measurements of the magnetic field, gave

$$P=3.835\pm0.006\times10^{-5}G^{-1}.$$

It is quite clear from Fig. 2 that these long periods arise from approximately cylindrical Fermi surfaces which are tilted in the yz plane. A separate experiment, in which the field was rotated in a plane containing the z axis but inclined at 15° to the yz plane, showed that the necks had no tilt in the xy plane. This also shows that their degeneracy is either three or six, and therefore that they do not lie at a general point in the Brillouin zone (see Ref. 4 for a detailed discussion).

The tilt angles and period maxima were found by making a least-squares fit of the observed periods to an expression of the form

$$P^2(\theta)=A+B\sin2\theta+C\cos2\theta, \qquad (3.1)$$

where θ is the angle from the z axis. In units of $10^{-10}G^{-2}$ the values obtained were $A=7.495$, $B=-2.534$, $C=7.195$, with a tilt of $-9.6\pm0.1°$ and $P_{\max}=3.89\pm0.01\times10^{-5}G^{-1}$ for the curve γ_1 in Fig. 2. For the other curve γ_2 the corresponding values were, in the same units, $A=7.252$, $B=1.247$, $C=7.433$, with a tilt of $+4.8\pm0.1°$ and $P_{\max}=3.85\pm0.01\times10^{-5}G^{-1}$. Clearly, these are the principal and nonprincipal branches,

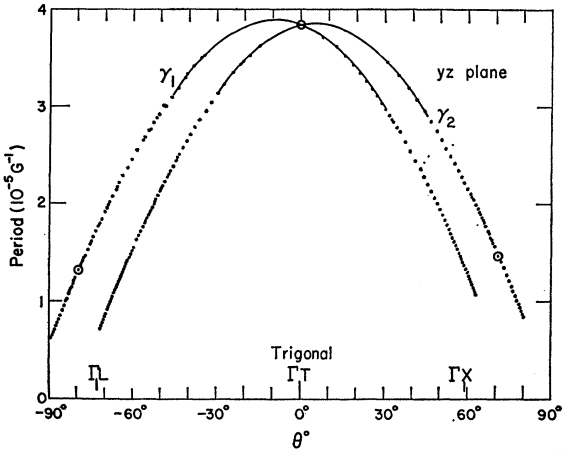

FIG. 2. The long periods observed in the yz plane. These are referred to in the text as the γ oscillations. The solid line is a hyperbolic fit using Eq. (3.1), with the parameters given in the text. Over the rest of the data the hyperbolic fit is within the experimental error. ⊙—points measured using NMR.

respectively, because application of a threefold rotation to the principal branch gives excellent agreement with the observed nonprincipal tilt angle and maximum period.

A most important feature of these surfaces is that they are necks. This is clear from the fact that $(B^2+C^2)^{1/2}>A$ and is illustrated by Fig. 3, in which the observed $(P_0\cos\Psi-P)$ for the principal neck is plotted against Ψ, where Ψ is the angle in the yz plane from the maximum period P_0. The period decreases more rapidly than $\cos\Psi$ for all Ψ, and this is characteristic of a neck.

B. The Short Periods

Figure 4 shows the short periods in the yz plane. These data fall into two distinct groups.

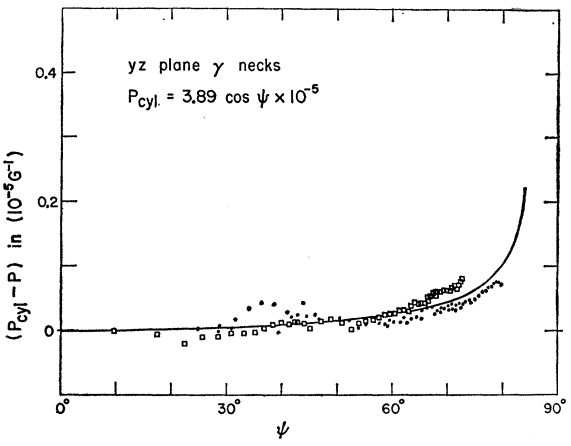

FIG. 3. The deviations of the observed principal γ-neck periods from a cylindrical approximation in the yz plane. Ψ is the angle from the period maximum at $\theta=-9.6°$; dots represent θ negative, squares represent θ positive. The solid line is the hyperbolic fit to Eq. (3.1).

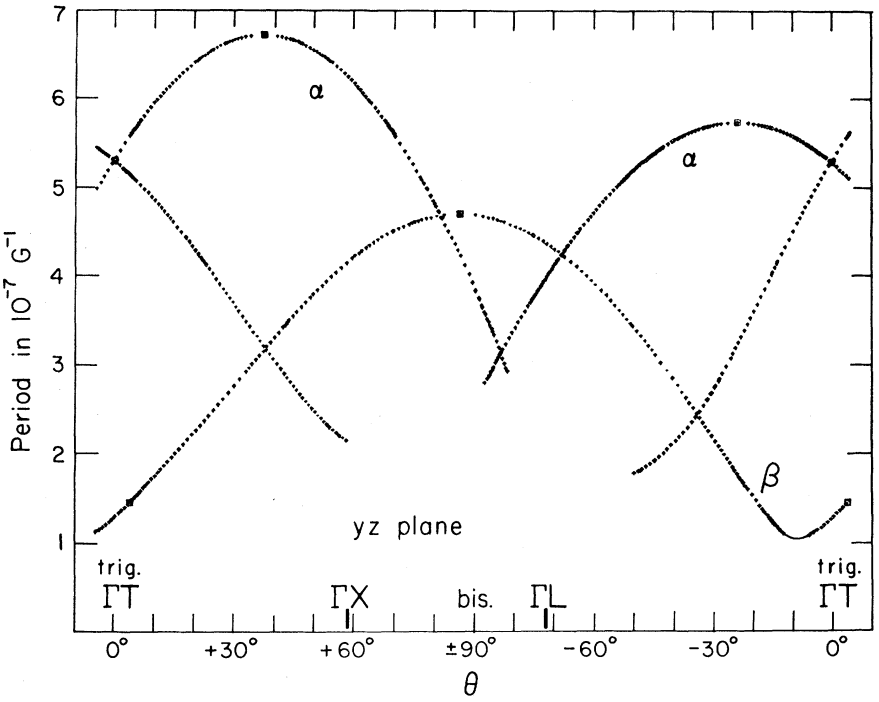

FIG. 4. The observed short periods in the yz plane. The extrapolated values of the β oscillations is shown near the trigonal axis. The squares are points checked by NMR.

(1) We shall call the first group the α carriers, with a principal pocket which has a maximum period of 6.715 $\pm 0.006 \times 10^{-7} G^{-1}$ at $+37.25 \pm 0.1°$ from the trigonal axis. The corresponding nonprincipal pockets have a maximum period of $5.735 \pm 0.006 \times 10^{-7} G^{-1}$ at $+156.15 \pm 0.1°$ from the trigonal axis. These are the Berlincourt carriers, and at first sight appear consistent with an approximately ellipsoidal model. However, there is one feature that strongly suggests a multiply connected surface, namely, that the α carrier oscillations disappear abruptly at certain orientations. A striking example of this is shown in the field-rotation diagram in Fig. 5, which shows the disappearance of the principal α oscillations in the yz plane at about $-81.8°$ from z, the trigonal axis. This recorder trace shows that the amplitude of the α oscillations decreases by a factor of at least 50 within 1° and then disappears. The only convincing explanation for this is that the corresponding extremal cross section ceases to exist. Similar behavior was observed at the other points in Fig. 3 where the data for the α carrier ceases.

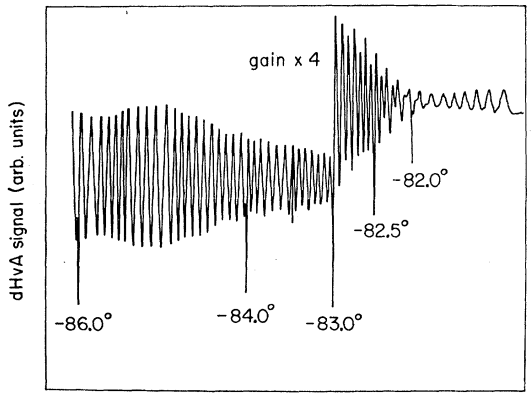

FIG. 5. Rotation data which show the abrupt disappearance of the α oscillations in the yz plane near the bisectrix axis. The angles θ are measured from the z axis. Note that the amplitude decreases by more than a factor of 50 within 1°. The small oscillations that remain at the right are due to another period.

(2) We shall call the other carrier the β carrier. In the yz plane this has a maximum period of $4.694 \pm 0.004 \times 10^{-7} G^{-1}$ at $+86.4 \pm 0.1°$ from the trigonal axis ΓT. We observe only the principal pocket of this set, probably because of the large angle between the oscillatory magnetization and the pickup-coil axis for the nonprincipal pockets. The β oscillations appear to come from a closed pocket and are observed over all the yz plane with the exception of a region of about 7° near the trigonal axis (Fig. 4). Here the amplitude does not decrease abruptly but falls gradually until it is below the noise level. In order to obtain a good estimate of the volume of each pocket of the β carriers it is therefore necessary to extrapolate the data to find both the position and magnitude of the minimum period. The best extrapolation functions are those which have the appropriate symmetry and periodicity for the yz plane and also form an orthonormal set. We therefore make a least-squares fit of all the principal β carrier data in the yz plane to a finite Fourier series of the form

$$P^2(\theta) = a_0 + \sum_{l=1}^{N} a_{2l} \cos(2l\theta) + b_{2l} \sin(2l\theta), \quad (3.2)$$

where θ is the angle from the trigonal ΓT.

We thus have $2N+1$ terms. We fit to $P^2(\theta)$, the square of the period, rather than directly to $P(\theta)$ because for an ellipsoid the expansion for $P^2(\theta)$ terminates after 3 terms. It was, however, necessary to use a large number of terms to obtain a good fit to the observed data. The final 35-term expansion (see Fig. 6 for details) gave an extrapolated period minimum of $1.045\pm0.005\times10^{-7}\mathrm{G}^{-1}$ at $-9.0\pm0.2°$ from the trigonal axis. It should be noted here that the two extrema of the period plot for the β carriers in the yz plane are not 90° apart, the angle between them being $84.6\pm0.2°$. This indicates that the corresponding pocket of the Fermi surface is somewhat S shaped in the yz plane.

Figure 7 shows the short period data in the xy plane. The α carriers are observed only within about 38.5° of the principal bisectrix direction, but the β carriers are found at all angles except for a region of about 5° either side of the principal binary axis. We again use a Fourier series to extrapolate the data to the binary axis, but now the expansion is simpler because the period curve has mirror symmetry about the binary axis. Thus we need only the cosine terms in the expansion of P^2 in Eq. (3.2). An 11-term extrapolation yields

$$P_{\text{binary}}=1.304\pm0.004\times10^{-7}\mathrm{G}^{-1}.$$

The rotation data for both the α and β carriers in the xy plane show that any tilt in the xy plane is less than 0.1°. Hence both are almost certainly 0° and consequently the number of pockets of these carriers is either three or six.

Another group of periods, which are labeled δ in Fig. 7, is found when the field lies within about 6° of the binary axis. These do not fit at all into the tilted "ellipsoid" schemes and it is shown below that they are a consequence of the multiply connected hole surface. Note that the data in Fig. 7 show unambiguously that the δ periods cross at the binary axis in the xy plane.

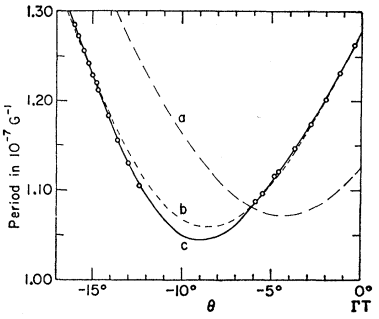

FIG. 6. Details of the extrapolation of the β period over the 7° region in the yz plane where no β oscillations were observed. The circles represent measured periods. The extrapolations are made by a least-squares fit to Eq. (3.2). Curve (a) has 3 terms (i.e., an ellipsoidal fit); curve (b) has 21 terms; curve (c) has 35 terms.

The data for the short periods in the xz plane are shown in Fig. 8. Those for the α carriers were obtained by field rotations and the expected three branches are seen. Again the α oscillations were found to disappear abruptly at certain orientations and these are shown in the figure. In this plane the β-carrier data are less accurate ($\pm1\%$) because they were obtained from field sweeps not directly calibrated by NMR. Only two of the three groups of β oscillations were found because the third has an oscillatory magnetization which is almost perpendicular to both the modulation

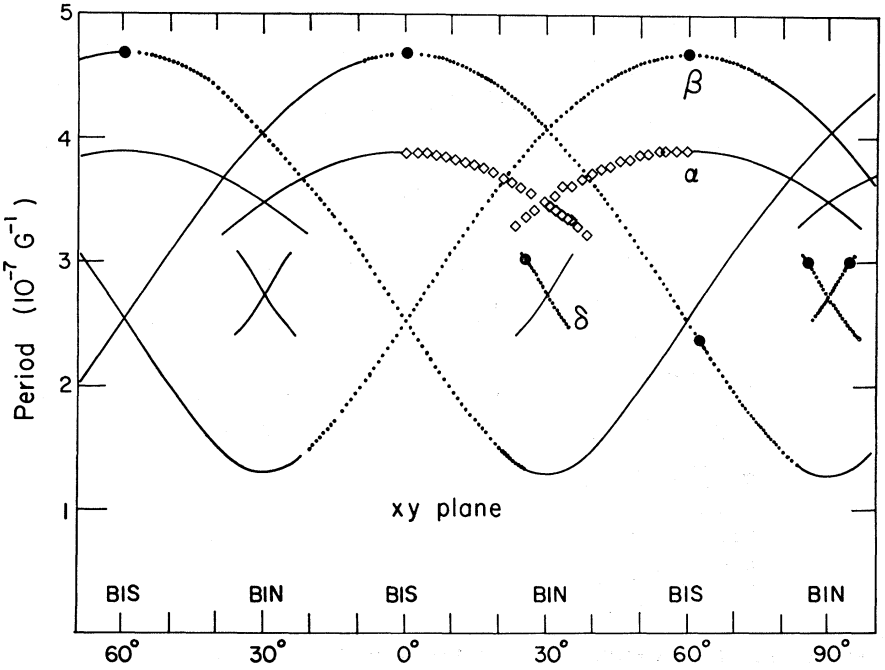

FIG. 7. The data for the short periods in the x-y plane. The data have mirror symmetry about the bisectrix and binary axes only if the field is rotated accurately in the xy plane. Large circles are points obtained from NMR measurements. The 11-term extrapolated values of the β period are shown.

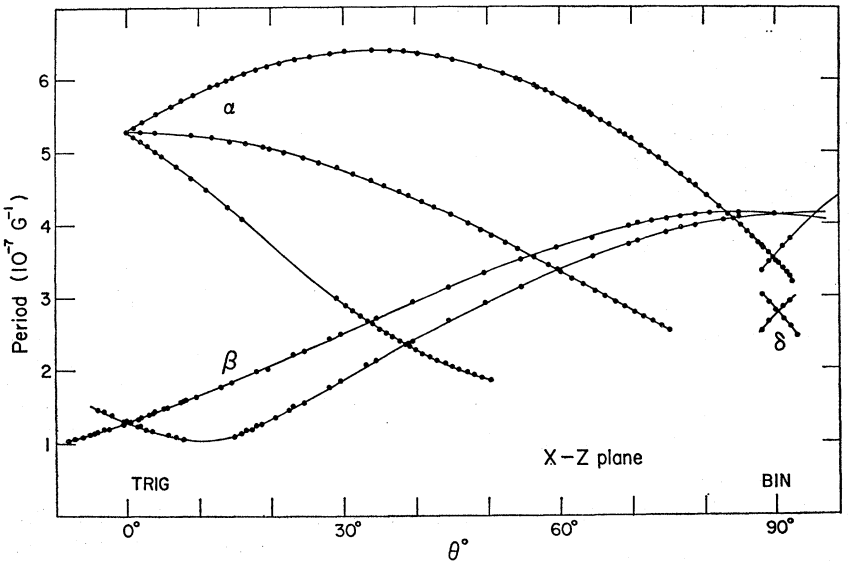

FIG. 8. The data for the short periods in the xz plane. In this plane the α-carrier data only were obtained by field-rotation measurements. The smooth curves are free-hand fits to the data.

coils and the pickup coil. The two observed sets of β oscillations are in agreement with the proposed model of three or six closed pockets.

When the field is within about 3° of the binary axis we again observe the δ oscillations and in this plane, too, we find that the δ periods cross at the binary axis. The corresponding Fermi surface orbits are thus skew in both the xy and yz planes.

A summary of the period data is given in Table I. A number of mixing frequencies were observed in all three planes. These were all accounted for as either the sum or difference of the observed dHvA frequencies and consequently are not shown as data in the figures.

In the remainder of this section we discuss in detail the angular variation of the α and β oscillations and we attempt to establish the necessary volume compensation by making a careful estimate of the volume of each pocket.

First we consider the α oscillations. In Fig. 9 we have collected together all the data on their angular range. These are shown on a stereogram centered on the field direction for the period maximum, i.e., +37.25° from ΓT in the yz plane. This figure illustrates the pronounced asymmetry in the angular range of the α oscillations in the yz plane, in that they extend for 87° from $P_{\max}$ in the direction to ΓT, but only for 61° towards ΓX. There is a corresponding asymmetry in the periods themselves, as is shown in Fig. 10(a), in which the deviations of the measured periods from the best ellipsoidal fit are plotted as a function of the angle from the period maximum. The best ellipsoidal fit is determined in the same arbitrary but plausible way as in Ref. 4, i.e., the best extrapolated values of the extremal periods are taken as the principal ellipsoidal periods even though the former are not 90° apart. Figure 10(a) also shows the 21-term least-squares fit to Eq. (3.2) and this is clearly an excellent fit to the data.

TABLE I. Arsenic data summary (a.u.=atomic units).

	Bisectrix trigonal plane (yz)		Binary axis (x)
α oscillations			
Maximum period in 10^{-7}G^{-1}	6.715±0.006		
Extremal area in 10^{-3} a.u.	3.981±0.004		
Tilt from trigonal ΓT	+37.25 ±0.1°		
β oscillations			
Extremal periods in 10^{-7}G^{-1}	4.694±0.004	1.045±0.005[a]	1.304±0.004[b]
Extremal areas in 10^{-3} a.u.	5.695±0.005	25.5 ±0.1	20.50 ±0.07
Tilt from trigonal	+86.4 ±0.1°	−9.0 ±0.2°[a]	
γ oscillations			
Maximum period in 10^{-5}G^{-1}	3.89±0.01		
Minimum area in 10^{-5} a.u.	6.87±0.02		
Tilt from trigonal	−9.6 ±0.1°		
δ oscillations			
period in 10^{-7}G^{-1}			2.76 ±0.01
area in 10^{-3} a.u.			9.68 ±0.03

[a] 35-term extrapolation over 3.1°. [b] 11-term extrapolation over 4.7°.

We now need to estimate the volume of an α pocket. Because these are so nonellipsoidal and because (as is shown below) they lack a center of symmetry, any estimate will be subject to considerable and unknown systematic error. A reasonable way[4] to calculate the volume is to take the three extremal periods and to use these in the expression for the volume of an ellipsoidal pocket

$$V=(8/3\pi^{1/2})(e/ch)^{3/2}(P_1P_2P_3)^{-1/2} \text{ carriers/cm}^3. \quad (3.3)$$

This can be seen to give good results when the pockets are only slightly nonellipsoidal. In our case we do not observe three extremal periods for the α carriers because the pockets are multiply connected, so the best we can do is to find extrapolated values, which do not, however, imply the existence of a corresponding extremal area. In the yz plane a 21-term extrapolation using the method described earlier gives a minimum period of $1.60\times10^{-7}\text{G}^{-1}$ at $-64°$ from the trigonal axis. In the xy plane the data must be extrapolated for over 50° and the simple two-term fit to the observed data shown in Fig. 10(b) gives $P_{\text{bin}}\simeq1.75\times10^{-7}\text{G}^{-1}$. When these values are substituted in Eq. (3.3) we find that the number of carriers per pocket is 3.9×10^{19} cm^{-3}.

Fortunately the analysis of the β-carrier data is much simpler, because the β pockets are closer to ellipsoids and the data cover nearly the whole range of angles. However, the pockets are still nonellipsoidal, as is shown by Fig. 11(a), in which the deviations from the best ellipsoidal fit in the yz plane are shown as a function of the angle from the period maximum. A corresponding plot for the xy plane is shown in Fig. 11(b).

For the β carriers we expect to be able to obtain a much more reliable estimate of the volume of each pocket by using the ellipsoidal formula (3.3), with the three principal extremal periods obtained earlier in this section. We thus find that the volume per β pocket

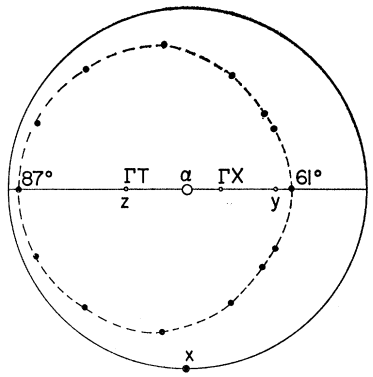

FIG. 9. A stereogram showing the angular range of the α oscillation. It is centered on the period maximum in the yz plane at 37.25 $\pm0.1°$ from the trigonal direction ΓT. Closed circles are the observed disappearances of the α oscillations in the principal planes.

corresponds to $(7.07\pm0.04)\times10^{19}$ carriers/cm^3, where the error shown represents just that due to the random errors in the determination of the principal periods. The ratio of the volume of a β pocket to that of an α pocket is therefore 1.8, with an error which we guess to be of the order of 20%. This large error arises almost entirely from the difficulty in estimating the volume of an α pocket. It is shown below that the γ necks are associated with the α pockets, but in any case, they make only a negligible contribution to the volume.

The actual value of this ratio must of course be a simple rational number. The nearest remaining possibilities are 1, 2, and 4, so it is natural to conclude that the real value of the ratio is 2. Even though our estimate of the volume of an α pocket may not be very accurate, we feel that it is sufficiently good to rule out any other value for the volume ratio.

It now follows that, since neither set can contain twelve pockets, there are six α pockets and three β pockets, hence the β pockets must be located at either the point L or X in the Brillouin zone. Both of these points are a center of symmetry, so we have now shown that the corresponding β surface is centrosymmetric,

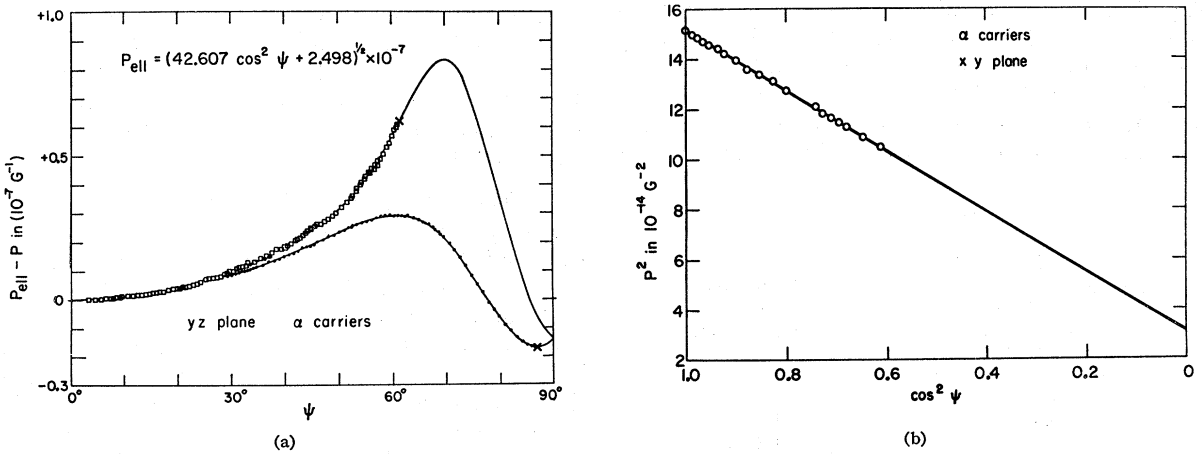

FIG. 10. (a) The deviations from ellipsoidal behavior shown by the α oscillations in the yz plane. $\Psi=0$ is the period maximum at $\theta=37.25°$ from z, the trigonal axis. Closed circles are periods for $\theta<37.25°$; squares are periods for $\theta>37.25°$; × marks the sharp disappearance of the α oscillations. The solid line is the 21-term fit to the data, using Eq. (3.2); this is used in the volume estimate. (b) A plot of P^2 versus $\cos^2\gamma$ for the α oscillations in the xy plane; $\Psi=0$ is the bisectrix axis. The straight line is the least-squares fit mentioned in the text.

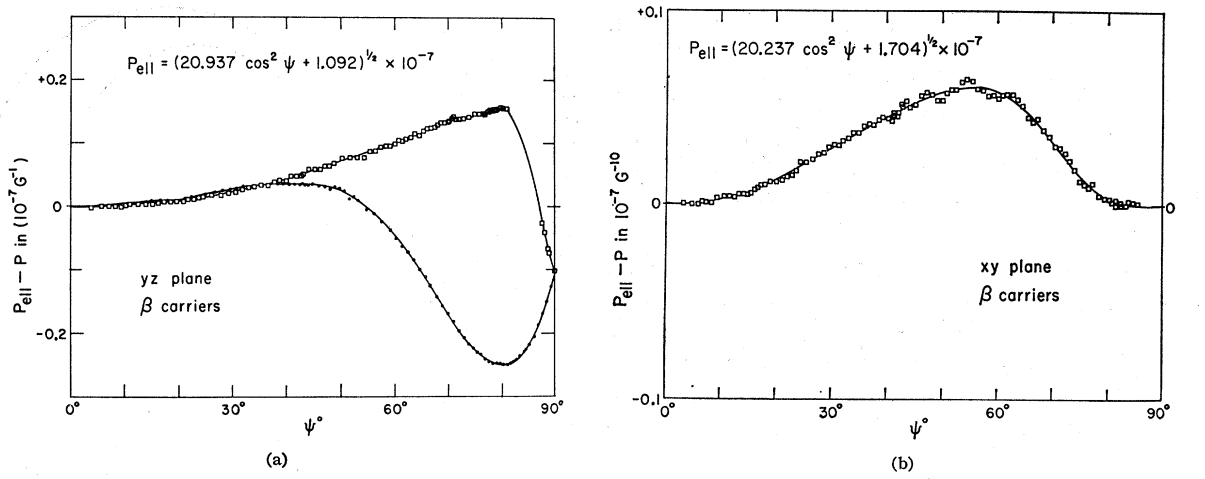

FIG. 11. (a) The deviations of the β periods from ellipsoidal behavior in the yz plane. $\Psi=0$ is the period maximum at $+86.4°$ from the trigonal axis. Closed circles are periods for $\theta<86.4°$, squares are periods for $\theta>86.4°$. The solid line is the least-squares 35-term fit to the β periods, using Eq. (3.2). (b) A similar plot for the xy plane. $\Psi=0$ is at the bisectrix axis. The solid line is the 11-term fit to Eq. (3.2) used in the volume estimate.

and hence that its extremal area is always the central section. This removes the major source of uncertainty in the extimation of its volume and shows that the quoted volume of $(7.07\pm0.04)\times10^{19}$ carriers/cm^3 is not subject to any major systematic error. Since there are three β pockets the total number of carriers of each sign is $(2.12\pm0.01)\times10^{20}$ per cm^3.

Several measurements of the effective mass were made, in order to permit estimates of the relevant Fermi energies. The temperature variation of the oscillation amplitude was measured and the standard amplitude expression[15] was used to derive the cyclotron mass. The values found are listed in Table II together with estimates of the Fermi energies derived from a parabolic band approximation. This approximation is reasonable for the β pockets, but may be rather poor for the α pockets because of their large deviations from ellipsoids. Comparison with the fragmentary cyclotron-resonance data[12] is inconclusive. Datars and Vanderkooy measured (to $\pm10\%$) effective masses of 0.16 and 0.33 for $\mathbf{H}\|x$, and 0.14 and 0.22 for $\mathbf{H}\|y$. The values of 0.14 and 0.16 agree with the predictions from our measured masses for the β pocket and the value of 0.22 for $\mathbf{H}\|y$ is probably due to the principal α pocket. The mass of 0.33 found for $\mathbf{H}\|x$ is probably the δ period, although our measurements give 0.26 ± 0.01 for this period.

TABLE II. Measured effective masses m^*/m_0.

γ neck for $\mathbf{H}\|$trigonal	0.028 ± 0.001
β pocket for $\mathbf{H}\|$minimum area	0.130 ± 0.005
α pocket for $\mathbf{H}\|$minimum area	0.098 ± 0.005
δ oscillations at binary	$0.26\ \pm0.01$
Fermi energies derived in a parabolic approximation	ϵ_F(Ry)
γ neck	7.8×10^{-4}
β pocket	1.4×10^{-2}
α pocket	1.3×10^{-2}

[15] I. M. Lifshitz and A. M. Kosevich, Zh. Eksperim. i Teor. Fiz. 29, 730 (1955) [English transl.: Soviet Phys.—JETP 2, 636 (1956)].

IV. INTERPRETATION AND COMPARISON WITH OTHER EXPERIMENTS

In this section we discuss the arrangement in the Brillouin zone of the pieces of Fermi surface described by the data given in the previous section.

Our observation that the long γ periods are in fact necks shows that they connect at least two larger pieces of surface. Since the α carriers show features characteristic of multiply connected surfaces we conclude that the α oscillations arise from the pockets which the necks connect. We have already shown that there are six α pockets, three β pockets, and either three or six γ necks.

Before discussing the arrangement of the α pockets we make some preliminary remarks about the origin of the δ oscillations. Since the β carriers form a simple set of closed surfaces it is natural to conclude that the δ oscillations come from the same surface as the α and γ oscillations. The crossing of the δ oscillations at the binary axis in both the xy and xz planes shows that:

(a) The δ orbit cannot be centered on the binary axis perpendicular to it, because that would require each period branch to be symmetric about that axis. The same argument shows that the δ orbit does not lie in the mirror plane.

(b) The δ oscillations are twofold degenerate at each binary axis. There are three distinct binary axes, so there are six different δ periods. The number of orbits is thought to be twice this because of the inversion symmetry about Γ or T. The δ orbits are thus skew in both planes.

The observation that the area of a δ orbit is larger than that of the parallel α orbit together with the fact

that the α orbit is a local maximum in the cross-sectional area shows that the δ orbit cannot be a topologically equivalent maximum area. No other period is observed which could provide the necessary intermediate minimum cross section, so it follows that (1) the α and δ orbits are topologically distinct, and (2) that the δ orbit arises from a skew orbit associated with the junction of the γ necks and the α pockets.

We now return to the problem of the arrangement of the α pockets and make the further plausible assumption that any surface they form is completely describable in terms of smooth α pockets connected by γ necks. This assertion is supported by the carrier compensation derived in Sec. III and by the smooth behavior of the α periods.

The only possibilities are that the α pockets are connected in groups of two, three, or six, and we consider these in turn.

If we have groups of two, there must be three such groups. This follows from the observed zero xy tilt for the α pockets and is independent of our arguments based on volume compensation. Each group of two pockets is therefore centered on an inversion center. The four inversion centers are Γ, T, L, and X. The first two are obviously ruled out because there would not be enough pockets and because there would then be no yz tilt for either the α or γ periods. The remaining points, L and X, lie in the mirror plane, so that the α pockets and the associated γ necks would then lie in this same vertical plane. If this were so we could find no explanation for the skew nature of the δ periods, so we discard groups of two.

Because of the limitations placed by the available point-group symmetries, groups of three can themselves exist only in inversion pairs above and below Γ or T. These points have symmetry $\bar{3}m$ and it is easily seen that for groups of three pockets this requires that the tilt angles of the γ necks be 90°. This contradicts the data and we therefore are left with one group of six α pockets as the only remaining possibility. Since neither the α nor the γ oscillations have any xy tilt, it follows that in a projection perpendicular to ΓT, the γ necks lie at 60° to the α pockets they connect. The resultant complex surface then has just two possible locations in the Brillouin zone, around Γ or around T. Both of these have the point group symmetry $\bar{3}m$ and the dHvA data cannot distinguish between them. In both these cases we have six α pockets and six γ necks.

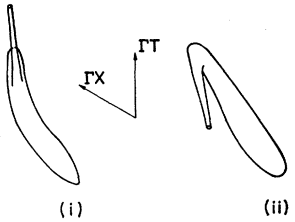

FIG. 12. Two possible arrangements of the α pockets and the γ necks.

The present data also enable us to determine some further features of this surface. We know that the six γ necks must be either centered on the binary axis or lie in the mirror plane, but it is clear that the second of these possibilities does not fit the data, because then there would be either too many α pockets or there would also be another no-tilt pocket at Γ or at T, and this is not observed experimentally. We thus conclude that the α pockets lie in the mirror plane and that the γ necks are centered on the binary axes. The surface is thus multiply connected, with the topology of a torus.

It now remains to determine the relative orientation of the α pockets and γ necks. The data show that their tilt angles are of opposite sign and this restricts us to the two possibilities shown in Fig. 12.

We distinguish between these by using the measured asymmetry of the α periods in the yz plane. This was discussed in Sec. III and it is evident that the pronounced asymmetry of the angular range in the yz plane (Fig. 9) of the α period with respect to its period maximum is consistent with arrangement (i) in Fig. 12, but not with arrangement (ii), because the latter would predict an asymmetry of the opposite sign to that observed.

We have thus shown that consideration of the experimental data alone leads to the conclusion that the α, γ, and δ oscillations are all due to a complex multiply connected surface of symmetry $\bar{3}m$ about Γ or T. The surface consists of six γ necks (with a tilt of $-9.6°$) centered on the binary axes through Γ or T and six α pockets (with a tilt of $+37.25°$) which lie in the mirror plane through ΓT. These are connected by six γ necks as shown in Fig. 13. Three of the pockets lie above the plane perpendicular to ΓT through the inversion center, and the other three lie below in the remaining sextants.

No other arrangement is consistent with our experimental data. We have previously established that these six α pockets, together with three closed β pockets, give satisfactory volume compensation if one set are electrons and the other are holes, but of course the dHvA data alone do not tell us which is which. Fortunately, the identification is self-evident when we compare the dHvA data with the pseudopotential band calculation of Falicov and Lin, as is done in Sec. V.

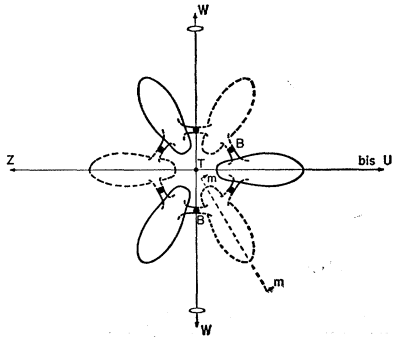

FIG. 13. A projection of the multiply connected hole surface on the binary-bisectrix plane through T. The shaded circles B are the intersection of the surface with this plane. The full lines denote projection from above; the dotted lines projection from below.

TABLE III. Arsenic electrons. Areas and masses are given in atomic units.

	This experiment β carriers	Pseudopotential calculation (Lin and Falicov)
Number of pockets	3	3
Location in Brillouin zone	L or X	L
Tilt in yz plane for:		
(a) minimum area	$+86.4\pm0.1°$	$\sim+80°$
(b) maximum area	$+171.0\pm0.2°$	$\sim+171°$
Minimum area for **H** in yz plane	$(5.695\pm0.005)\times10^{-3}$	5.5×10^{-3} [a]
Area for **H**$\|\|$ to x (binary)	$(2.050\pm0.007)\times10^{-2}$	1.8×10^{-2}
Area for $H\|\|$ to z (trigonal)	$(2.088\pm0.005)\times10^{-2}$	1.6×10^{-2}
Total number of electrons	$(2.12\ \pm0.01)\times10^{20}$ cm^{-3} $(4.60\ \pm0.05)\times10^{-3}$ per atom	
Principal effective masses in ellipsoidal approximation		
(a)along binary axis	0.163	0.11
(b)in yz plane	0.105	0.038
	2.11	0.94
Fermi energy (Ry)	0.0140 [b]	0.0270

[a] The electron Fermi energy was fitted to this value. [b] Derived in a parabolic approximation.

We have still to establish the details of the origin of the δ oscillations, which have been shown to arise from a skew orbit associated with the junction of the γ necks and the α pockets. The most likely assignment appears to be that shown in Fig. 14, and this is supported by consideration of the values of $dP/d\theta$ shown by the δ periods at the binary axis. These give us a direction associated with the surface traced out by the orbit. It is clear that the relation is exact only for a cylinder, but the concept remains useful in a more general case. The "angle of tilt" (in the above sense) is given by

$$\varphi=\tan^{-1}[(1/P)(dP/d\theta)].$$

For the δ oscillations with **H** parallel to x these angles are 51° and 70° in the xy and xz planes, respectively, measured from the binary axis. These magnitudes are reasonable for the interpretation given in Fig. 14. In particular we note that the tilt in the xz plane (when referred to the trigonal axis ΓT) should be intermediate between the principal α tilt of 37.25° and the non-principal γ tilt of 4.8°. The δ value of 20° satisfies this condition. The relative signs of these two angles for an individual δ period are also relevant, but they have not been determined experimentally.

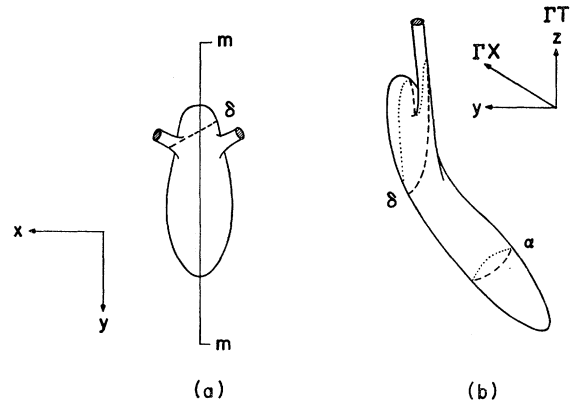

FIG. 14. Two sketches to show the proposed origin of the δ period. (a) One α pocket is shown in the same projection as Fig. 13. (b) The section of an α pocket by the mirror plane. This is shown as section mm in Fig. 13.

There is one shortcoming in this interpretation of the experimental data, in that it necessarily predicts an extra extremal area for **H** parallel to the binary axis. This extremal lies in the mirror plane σ and is the central section of an α pocket. A careful search was made for this missing period, but it was not observed. We assume that this is because it has a very low amplitude, and a plausible reason for this is the expected large curvature of this α surface perpendicular to the central orbit for this particular field direction.

As an over-all check on our interpretation we may use this model to calculate the electronic specific heat, which has recently been measured by Culbert.[16] He finds $\gamma_{el}=0.194\pm0.007$ mJ mole^{-1} °K^{-2} for arsenic. For ellipsoidal parabolic bands we may write the coefficient of the linear term in the specific heat as

$$\gamma_{el}=\tfrac{1}{2}\pi^2k^2V\sum\frac{n}{\epsilon_F}\text{ per mole},$$

where V is the molar volume, n is the number of carriers/cm^3 per pocket, ϵ_F is the Fermi energy of a pocket, and the summation is over all pockets, both electrons and holes. We take six α pockets and three β pockets, with the parameters taken from Tables III and IV, and we treat the necks as cylinders with a length estimated from the observed angular range of the γ period. Although the necks make a negligible contribution to the volume, they make approximately an 8% contribution to the electronic specific heat, because their Fermi energy is so much smaller. Our calculated value for γ_{el} is 0.192 mJ mole^{-1} °K^{-2}, which is in surprisingly good agreement with the measured value of 0.194. This comparison provides strong support

[16] H. V. Culbert, Bull. Am. Phys. Soc. **10**, 1104 (1965).

TABLE IV. Arsenic holes. Areas and masses are given in atomic units.

	This experiment	Pseudopotential calculation (Lin and Falicov)
(1) γ necks		
Number:	6	6
Location in BZ	on binary axis through Γ or T	on binary axis through $T(TW)$
Tilt from ΓT in yz plane	$-9.6\pm0.1°$	$\sim-11°$
Minimum area	$(6.87\pm0.02)\times10^{-5}$	6.9×10^{-5} [a]
Minimum effective mass	0.028 ± 0.001	...
Fermi energy (rydbergs)	7.8×10^{-4} [b]	...
(2) α pockets		
Number:	6	6
Location in BZ	in mirror plane through Γ and T	near T in mirror plane through Γ and T
Minimum area in yz plane	$(3.981\pm0.004)\times10^{-3}$	difficult to calculate
Tilt angle of minimum area	$+37.25\pm0.1°$	$\sim+44°$
Fermi energy (Ry)	0.013 [b]	$\sim$0.0266

[a] The Fermi energy for holes was adjusted to fit this value. [b] Derived in a parabolic approximation.

for our previous conclusion that there are six α pockets and three β pockets.

The geometric resonance data[10] provide an additional check on our data. The β carriers have sufficient symmetry to ensure that the momenta observed for $q\|x$ and $\mathbf{H}\perp\mathbf{q}$ trace out the section of the Fermi surface which lies in the mirror plane. Thus, Fig. 2 of Ref. 10 gives directly the extremal dHvA area for $\mathbf{H}\|x$. These geometric resonance data give an area of $19.9\pm1.0\times10^{-3}$ a.u. which is in good agreement with our dHvA value of $20.50\pm0.07\times10^{-3}$ a.u.

V. COMPARISON WITH THEORY

A general survey of the band structures of the Group-V semimetals was recently made by Cohen, Falicov, and Golin.[2] They pointed out the primary role of the $A7$ crystal structure and showed that arsenic, antimony, and bismuth were likely to have rather similar band structures, with the holes at or near T and the electrons at or near L or X. A more detailed pseudopotential calculation for arsenic by Falicov and Golin[13] derived its pseudopotential by a four-parameter interpolation between the best values for Ge determined by Brust.[17] (Ge is next to As in the periodic table.) These four parameters were then varied a little in an attempt to fit the existing experimental data and the effects of spin-orbit coupling were added as a perturbation. Unfortunately, the then available experimental data were not enough to either identify the observed carriers or to establish a best choice of pseudopotential parameters. This work also concluded that the over-all features of the band structure were determined mainly by the crystal structure, while changes in the pseudopotential had relatively little effect.

A first-principle self-consistent orthogonalized-plane-wave (OPW) calculation was made by Golin[18] and this confirmed the general features of the pseudopotential calculation. However, it was not possible to identify the observed carriers or to calculate the expected tilt angles.

The appearance of further experimental data[10,11,19] prompted Lin and Falicov[14] to make further pseudopotential calculations and they were able to find modified pseudopotential parameters which gave an excellent fit to all the data. The calculation was carried out concurrently with this experiment and was in part guided by its preliminary results. In particular, our data showed that it was necessary to consider points of lower symmetry than in the earlier calculation.

The band structure finally obtained from this semi-empirical calculation is in excellent agreement with so many features of our experimental data that little doubt remains of its correctness near the Fermi level. The gross features of the band structure are very similar to the previous calculations but the details of the levels near L and T are rather different. The relevant levels are shown in Fig. 15. It should be noted that the maximum energy in the hole band lies on none

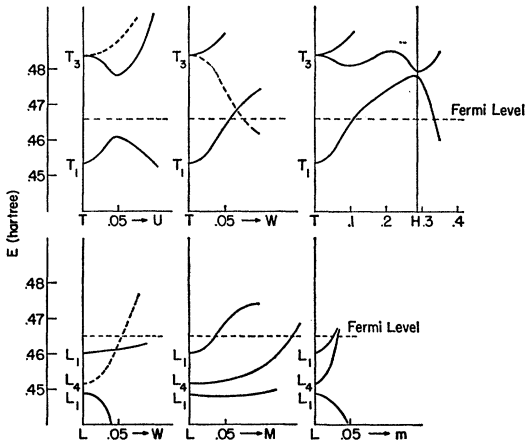

FIG. 15. Lin and Falicov's band structure for arsenic in the neighborhood of the points T (holes) and L (electrons). Energy and k vectors are given in atomic units.

[17] D. Brust, Phys. Rev. **134**, A1337 (1964).
[18] S. Golin, Phys. Rev. **140**, A993 (1965).
[19] M. G. Priestley, L. R. Windmiller, J. B. Ketterson, and Y. Eckstein, Bull. Am. Phys. Soc. **10**, 1089 (1965).

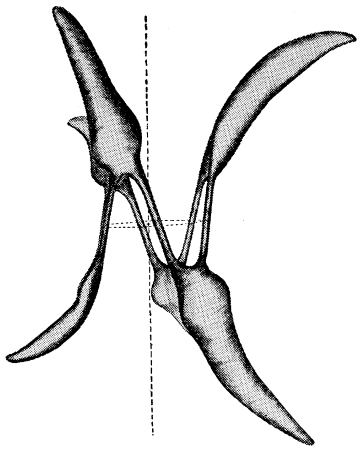

FIG. 16. A perspective view of the multiply connected hole surface as determined by Lin and Falicov's calculation.

of the symmetry lines through T but is in the mirror plane at a point H with rectangular coordinates $g_0(0.3595, 0.0027, 0.3595)$. (See Ref. 13 for the coordinate system and the value of g_0.) The six resultant pockets are joined by six necks centered on the TW line (the binary axis through T) and together form the complex hole surface sketched in Fig. 16. It is evident that this is in all essentials identical to that found from our experiment, except that this calculated Fermi surface would not produce the observed δ oscillations. The difference from the experimental Fermi surface is only a minor one and can be removed by making the γ necks join the α pockets a little away from the ends of the latter, as shown in Figs. 13 and 14. It is not clear whether minor changes in the pseudopotential parameters will remove this small discrepancy.

The electrons are in three closed pockets at the points L, the centers of the hexagonal faces not perpendicular to the trigonal axis (Fig. 1). A detailed numerical comparison between our experimental data and these calculations is shown in Tables III and IV, which cover electrons and holes, respectively.

The dHvA data for the pure metal of course give us no information about the signs of the carriers, but the comparison with the calculations gives an obvious choice of the three closed β pockets as electrons, while the complex multiply connected surface contains all the holes.

The agreement for the numbers of pockets and their Brillouin-zone locations is complete. The tilt angles agree very well in both magnitude and sign, and the general anisotropy of the pockets is correctly calculated. There is a minor disagreement in the electron effective masses, where the calculated values are approximately a factor of two too small, but this may well be due to the nonparabolic bands.

It is interesting to note that the locations and tilt angles of the carrier pockets are very similar to those for antimony.[3,4,6] There the electron pockets are also at L with a tilt angle only 1.1° larger than in arsenic, while the holes are again in a group of six about T. The spin-orbit coupling is larger in antimony and this may well account for its smaller number of carriers[4] (5.5×10^{19} electrons/cm^3) and the absence of the necks. Presumably in bismuth the spin-orbit coupling is so large that the maximum in the hole band lies directly at T and the resultant single-hole surface has no tilt.[7,8,20]

ACKNOWLEDGMENTS

We are grateful for stimulating discussions with Professor L. M. Falicov and Dr. P. J. Lin.

[20] R. N. Zitter, Phys. Rev. **127**, 1471 (1962).